Photoexcitation of a Dipole-Forbidden Resonance in Helium

B. Krässig,[1] E. P. Kanter,[1] S. H. Southworth,[1] R. Guillemin,[2] O. Hemmers,[2]
D. W. Lindle,[2] R. Wehlitz,[3] and N. L. S. Martin[4]

[1]*Argonne National Laboratory, Argonne, Illinois 60439*
[2]*Department of Chemistry, University of Nevada, Las Vegas, Nevada 89154*
[3]*Synchrotron Radiation Center, University of Wisconsin, Stoughton, Wisconsin 53589*
[4]*Department of Physics and Astronomy, University of Kentucky, Lexington, Kentucky 40506*

(Received 13 December 2001; published 2 May 2002)

We have observed photoexcitation of the dipole-forbidden $1s^2\,{}^1S_0 \rightarrow 2p^2\,{}^1D_2$ resonance in helium by measuring the nondipolar forward-backward asymmetry of photoelectron angular distributions in the $2\ell 2\ell'$ autoionizing region. By exploiting the electric dipole-quadrupole interference in the excitation of both the $2s2p\,{}^1P_1$ and $2p^2\,{}^1D_2$ levels, we have observed the quadrupole resonance in photoabsorption and extracted its Fano line shape parameters and the relative phase of the $1sEp$ and $1sEd$ continua. We find the quadrupole line profile index q_2 to be markedly different from theoretical expectations.

DOI: 10.1103/PhysRevLett.88.203002 PACS numbers: 32.80.Dz, 32.80.Fb

The autoionizing states of He have been studied in great detail for nearly 40 years. In fact, the pioneering work of Madden and Codling [1] on the doubly excited autoionizing states of He is generally considered to mark the dawn of the synchrotron radiation era in atomic physics [2]. In recent years, a substantial increase in the level of understanding of the excitation and decay of many Rydberg series of those resonances has been achieved [3–5]. All of that work, however, has been limited to $J = 1$ dipole-excited resonances. And although there have been systematic studies of the higher multipole resonances by electron impact [6–8], those resonances have never before been observed in more selective photoionization experiments. Recently, it was shown that because of the interference of a dominant $J = 1$ continuum with a weaker $J = 2$ resonance, it is possible to observe quadrupole resonances in photoabsorption by measuring photoelectron angular distributions [9,10]. In helium the autoionizing levels $2s2p\,{}^1P_1$ and $2p^2\,{}^1D_2$ lie close together at about 60 eV above the $1s^2\,{}^1S_0$ ground state. They are accessible by an electric dipole and electric quadrupole transition and autoionize into the $1sEp\,{}^1P_1$ and $1sEd\,{}^1D_2$ continua, respectively. In this work, we have carried out such an experiment in which we observe both the $2s2p\,{}^1P_1$ (dipole) and $2p^2\,{}^1D_2$ (quadrupole) autoionization resonances in He and determine the quadrupole resonance line shape parameters.

Interference between the electric dipole ($E1$) and electric quadrupole ($E2$) amplitudes produces a forward-backward asymmetry in photoelectron angular distributions with respect to the direction of the photon beam. For photoionization of the $1s^2\,{}^1S_0$ He ground state this asymmetry is characterized by the angular distribution parameter

$$\gamma = 3\alpha\omega\,\frac{\mathcal{R}_2}{\mathcal{R}_1}\cos(\delta_2 - \delta_1), \tag{1}$$

where α is the fine structure constant, ω is the photon energy, $\mathcal{R}_1, \mathcal{R}_2$ are the dipole and quadrupole radial matrix elements, and $\delta_{1,2}$ are the phase shifts of the Ep, Ed continuum states of photoelectron energy E [11,12]. Note that all quantities are in atomic units.

In regions of the photoionization spectrum where no autoionizing levels are present the quantities $\mathcal{R}_{1,2}$ and $\delta_{1,2}$ are all slowly varying functions of energy. When autoionization is present the general form of (1) remains the same, but these parameters are now strong functions of energy in the neighborhood of the resonances. Fano [13] showed that for a single autoionizing resonance coupled to a single continuum, the transition amplitude should be multiplied by the factor $(q + \varepsilon)/(i + \varepsilon)$. Labeling resonant quantities with the superscript R and the channel $\ell = 1, 2$ the resulting radial matrix elements and phases can be expressed as

$$\mathcal{R}_\ell^R = \mathcal{R}_\ell\,\frac{(q_\ell + \varepsilon_\ell)}{(1 + \varepsilon_\ell^2)^{1/2}} \tag{2a}$$

and

$$\delta_\ell^R = \delta_\ell + \Delta_\ell\,, \tag{2b}$$

where q_ℓ is the Fano line profile index and $\varepsilon_\ell = (\omega - \omega_\ell)/(\Gamma_\ell/2)$ is the energy with respect to the resonance position ω_ℓ measured in units of the halfwidth $\Gamma_\ell/2$ of the resonance. The extra phase shift due to autoionization Δ_ℓ is defined by $\cot\Delta_\ell = -\varepsilon_\ell$. Using these equations, the well-known form of the resonant cross section is given by

$$\sigma_\ell^R = \sigma_\ell\,\frac{(q_\ell + \varepsilon_\ell)^2}{(1 + \varepsilon_\ell^2)}\,. \tag{3}$$

Substituting Eqs. (2) into Eq. (1) gives the resonant value of γ^R in terms of γ_0, the value of γ defined by Eq. (1) that would exist at ω in the absence of any resonances as

$$\gamma^R = \gamma_0\left\{\frac{\cos(\delta_2 - \delta_1 + \Delta_2 - \Delta_1)}{\cos(\delta_2 - \delta_1)}\right\} \times \left\{\frac{(q_2 + \varepsilon_2)}{(1 + \varepsilon_2^2)^{1/2}}\right\} \Big/ \left\{\frac{(q_1 + \varepsilon_1)}{(1 + \varepsilon_1^2)^{1/2}}\right\}. \tag{4}$$

Experimental measurements of photoelectron angular distributions generally require accurate knowledge of the photon polarization properties [14]. To avoid this difficulty, we make use of a symmetry property of angular distributions noted by Peshkin [15], i.e., the average of two photoelectron intensities measured at the same polar angle with respect to the photon propagation direction $\boldsymbol{k}$ but differing by azimuthal angles of 90° is independent of polarization and equal to that for an unpolarized photon beam at that polar angle. We use four parallel-plate electron analyzers (PPAs) mounted on a rotation stage with its rotation axis perpendicular to $\boldsymbol{k}$. The two "forward" analyzers are positioned at 54.7° with respect to $\boldsymbol{k}$ and differ by 90° in azimuthal angle. The two "backward" analyzers are positioned at 125.3° with respect to $\boldsymbol{k}$ and also differ by 90° azimuthal angle. By averaging the photoelectron intensities in the two forward and two backward analyzers, we obtain signals that are independent of the photon polarization and the usual dipole anisotropy. The difference between the intensities in the forward and backward directions divided by their sum is proportional to γ and isolates the dependence of the angular distribution on the $E1$-$E2$ interference. For each photon energy, the rotation stage is rotated so that photoelectron intensities are measured by each analyzer at each of the four angles.

The experiment was performed on the PGM Undulator beam line at the University of Wisconsin's Synchrotron Radiation Center. The photon beam intersected an effusive gas jet at the common source point of the four PPAs and an ion detector recorded photoion yields. The PPAs were operated at a high pass energy of 100 eV with a nominal kinetic energy resolution of 2 eV. Variations of photoelectron intensities through the autoionizing resonances were measured by constant ionic state (CIS) scans in which the kinetic energies accepted by the PPAs were stepped along with the photon energy. The PPAs were then rotated and the CIS scan repeated. Four measurements of γ were determined from the four PPAs at each energy of the CIS scan, and the results were averaged to reduce systematic errors. The relative photoionization cross section through the resonance region was determined from the ion yield.

The experimental total cross section measurements are shown in the lower panel of Fig. 1. The well-known $(2s2p)\ ^1P_1$ resonance at 60.15 eV [4] is observed with its characteristic Fano profile [13] and was used to calibrate our absolute energies. The quadrupole resonance (weaker by $\alpha^2\omega^2 \sim 3 \times 10^{-4}$ relative to dipole) is not apparent in the total cross section. These data were fitted with a profile determined by the dipole cross section [Eq. (3)] convoluted with the ≈20 meV photon bandpass. The line shape of the bandpass function was determined in a separate measurement of the nearby xenon $4d \rightarrow 6p\ ^1P_1^o$ resonance at 65.11 eV [16]. Allowing the He dipole resonance width and q_1 to vary as free parameters, we obtain excellent agreement with the best values of those parameters available in the literature (see Table I). The quality of the fit with parameters consistent with previous measurements confirms our bandpass determination.

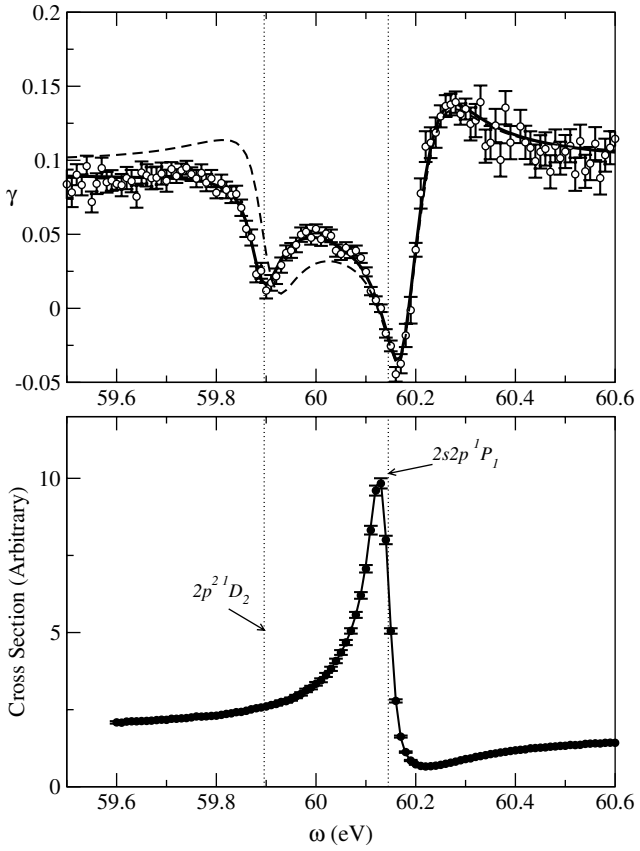

FIG. 1. Energy dependence of the cross section (bottom) and asymmetry parameter γ (top) in the region of the helium $(2s2p)\ ^1P_1$ and $(2p^2)\ ^1D_2$ autoionizing levels. The dashed curve shows the *a priori* prediction, using Eq. (4) and the theoretical parameters described in text and convoluted with the experimental resolution. The data and statistical errors are indicated in each figure as discrete points. Systematic effects are estimated to contribute ±0.02 to the error in the absolute value of γ. The fits, described in text, are shown as solid lines.

The upper panel of Fig. 1 shows the energy dependence of the parameter γ in the region of the helium $(2s2p)\ ^1P_1$ and $(2p^2)\ ^1D_2$ autoionizing levels. Although the quadrupole resonance is not observed in the cross section, it is clearly visible in the angular asymmetry. To fit these data, it is necessary to properly account for the photon bandpass. We do this by using Eqs. (3) and (4) and forming the convolution integrals of $\sigma_1^R(\omega)\gamma^R(\omega)$ and $\sigma_1^R(\omega)$. The convoluted $\overline{\gamma}^R$ is then defined by the ratio of those integrals.

Keeping the dipole resonance parameters fixed at the values determined from the cross section measurement, the data in Fig. 1 were best fitted with $\overline{\gamma}^R$ to yield the quadrupole resonance parameters shown in Table I. The resulting fit is shown in the upper panel of Fig. 1. The nonresonant asymmetry γ_0 was also determined from the fit and found to be 0.096(20) in good agreement with theoretical predictions [21,22]. The normalized χ^2 value for this fit was 0.93.

TABLE I. Helium autoionizing levels and relevant parameters obtained from the literature and present experimental results. The energies (ω_ℓ), widths (Γ_ℓ), and q_1 are prior experimental values [4,8]; q_2 [17,18] and the unperturbed continuum phase shifts (δ_ℓ) [19,20] are theoretical values.

	ℓ	ω_ℓ (eV)	Γ_ℓ (meV)	q_ℓ	$\delta_\ell - \delta_1$ (radians)
$2s2p\ ^1P_1$	1	60.150(4)	37.6(2)	−2.73(4)	0
This work			37.9(10)	−2.74(5)	
$2p^2\ ^1D_2$	2	59.91(2)	72(18)	−1.0	−0.3028
This work		59.905(5)	57(3)	−0.25(7)	−0.234(38)

Table I presents some previously reported experimental and theoretical values of the resonance parameters along with the present results. For the previous experimental values of the dipole resonance parameters, we show the results of the recent high-resolution study reported by Schulz *et al.* [4]. The quadrupole parameters for the energy and width are those reported by [8]. q_2 is taken from calculated values of the electron scattering quantity $q_2(K)$. In the limit of small momentum transfer K this is the same as the electric quadrupole value q_2; this follows from the fact that the Born radial matrix element in the spherical Bessel function $j_2(Kr) \propto r^2$ as $K \to 0$ [23]. The Born calculations by Lhagva and Hehnmedeh [17] and by Kheifets [18] are in good agreement yielding $q_2 \approx -1$. The Ep, Ed phase shifts have been calculated by Tweed and Langlois [19] and Lhagva [20] for various values of E; both calculations are in excellent agreement in the energy range of interest. The value $\delta_2 - \delta_1 = (-0.6315) - (-0.3287) = -0.3028$ in Table I was obtained by linear interpolation and is essentially constant over the autoionizing resonances. For comparison, these previous values were used to generate the dashed curve in Fig. 1 which clearly deviates from the measurements.

Our fitted values of Γ_2 and ω_2 represent a significant increase in precision over the previous experimental values shown in Table I. Recent theoretical works [24] converge on values of $\Gamma_2 = 64$ meV and $\omega_2 = 59.904$ eV. While the phase shift difference $(\delta_2 - \delta_1)$ we find only differs from the predicted value by less than 2σ, the shape parameter q_2 is substantially smaller in magnitude, suggesting near "window resonance" behavior. The fit shows a weak correlation between these two parameters. Further decreasing the phase shift to the theoretical value of $\delta_2 - \delta_1 = -0.3028$ would result in an even smaller magnitude of q_2 and further from the prediction. We note that a calculation by Jacobs [25] yielded values of q_2 at low (but nonzero) momentum transfer that may be compatible with our experimental result. The value of q_2 cannot be unambiguously determined from electron scattering experiments because all multipoles are present, affecting the line shape and the apparent value of q. Furthermore, the matrix elements which are probed in such experiments differ from the pure multipole matrix elements of photoabsorption [26].

Using the resonance parameters determined in the fits, we have computed the individual bracketed terms in Eq. (4) and show those in Fig. 2b. Whereas the energy dependence of the total cross section (bottom panel) is determined solely by the square of the dipole matrix element, that of the γ parameter is affected by the interplay among the phase shift difference and the matrix elements. These produce a local minimum in γ at the quadrupole resonance position. The γ at the quadrupole resonance shows a minimum of ~ 0 because both the $\mathcal{R}_2$ matrix element and phase shift terms in the numerator of Eq. (4) cross zero and change sign at ω_2 as a consequence of the small magnitude of q_2, and hence the product is always positive definite. At the energy $(\varepsilon_1 = -q_1)$ that the

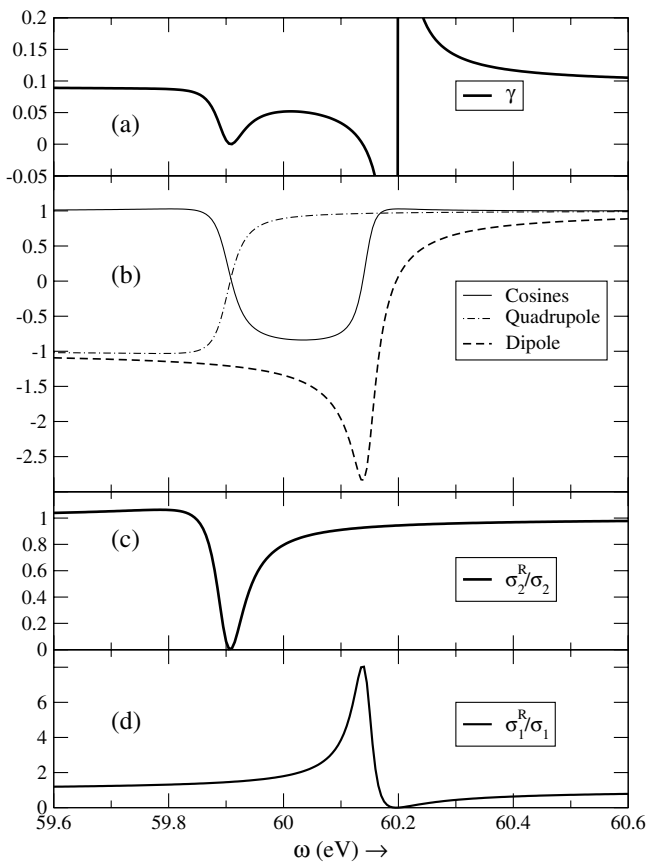

FIG. 2. Energy dependence of the various dimensionless terms in Eq. (4) computed using the fitted parameters. Panel (a) shows the value of γ computed with that equation while (b) shows the three bracketed ({}) terms in that equation. Panels (c) and (d) show the energy dependence of Eq. (3) for the quadrupole and dipole resonance cross sections, respectively.

amplitude of the dipole resonance passes through zero, the value of γ diverges and changes sign; in the experiment the finite energy resolution results in a finite measured quantity. The energy dependence of the quadrupole cross section (Fig. 2c) exhibits the characteristic dip of a window resonance.

Beyond demonstrating a method of observing higher multipole resonances in photoionization, a powerful feature of the present experiment lies in the ability to obtain not only the magnitude q_2 but also the relative phase $\delta_2 - \delta_1$ and matrix element ratio $\mathcal{R}_2/\mathcal{R}_1$. This is possible because of the strong energy dependence of γ^R [Eq. (4)]; away from resonance the form of γ [Eq. (1)] does not permit the separate determination of both magnitude and phase from experiment. (The technique of using the *shape* of an interference feature to obtain phase information has been used previously in an $(e, 2e)$ experiment [27].) The profile index q is determined by the ratio of the transition matrix elements for direct excitation of the resonance compared to that of the continuum [13] and thus serves as a probe of the electron correlation in the doubly excited resonance. The experimental values of these quantities presented here provide a rigorous test, not previously available, for He wave functions and calculations of dynamic processes.

This work was supported by the Chemical Sciences, Geosciences, and Biosciences Division of the Office of Basic Energy Sciences, Office of Science, U.S. Department of Energy, under Contract No. W-31-109-Eng-38. N. L. S. M. and the UNLV group acknowledge support by National Science Foundation Grants No. 9987861 and No. 9876996, respectively. We are grateful for the help and hospitality of the staff of the Synchrotron Radiation Center. The University of Wisconsin SRC is supported by National Science Foundation Grant No. DMR-0084402.

[1] R. P. Madden and K. Codling, Phys. Rev. Lett. **10**, 516 (1963).
[2] B. Crasemann and F. Wuilleumier, in *Physics of Atoms and Molecules,* edited by B. Crasemann (Plenum, New York, 1985).
[3] A. Menzel, S. P. Frigo, S. B. Whitfield, C. D. Caldwell, M. O. Krause, J.-Z. Tang, and I. Shimamura, Phys. Rev. Lett. **75**, 1479 (1995).
[4] K. Schulz, G. Kaindl, M. Domke, J. D. Bozek, P. A. Heimann, A. S. Schlachter, and J. M. Rost, Phys. Rev. Lett. **77**, 3086 (1996).
[5] M. K. Odling-Smee, E. Sokell, P. Hammond, and M. A. MacDonald, Phys. Rev. Lett. **84**, 2598 (2000).
[6] A. Crowe, D. G. McDonald, S. E. Martin, and V. V. Balashov, Can. J. Phys. **74**, 736 (1996).
[7] M. J. Brunger, O. Samardzic, A. S. Kheifets, and E. Weigold, J. Phys. B **30**, 3267 (1997).
[8] J. van den Brink, G. Nienhuis, J. van Eck, and H. Heideman, J. Phys. B **22**, 3501 (1989).
[9] N. L. S. Martin, D. B. Thompson, R. P. Bauman, C. D. Caldwell, M. O. Krause, S. P. Frigo, and M. Wilson, Phys. Rev. Lett. **81**, 1199 (1998).
[10] V. K. Dolmatov and S. T. Manson, Phys. Rev. Lett. **83**, 939 (1999).
[11] J. W. Cooper, Phys. Rev. A **47**, 1841 (1993).
[12] A. Bechler and R. H. Pratt, Phys. Rev. A **42**, 6400 (1990).
[13] U. Fano, Phys. Rev. **124**, 1866 (1961).
[14] M. Jung, B. Krässig, D. S. Gemmell, E. P. Kanter, T. LeBrun, S. H. Southworth, and L. Young, Phys. Rev. A **54**, 2127 (1996).
[15] M. Peshkin, in "Atomic Physics with Hard X-Rays from High Brilliance Synchrotron Light Sources," Argonne National Laboratory Report No. ANL-APS-TM-16, 1996, p. 207.
[16] D. L. Ederer and M. Manalis, J. Opt. Soc. Am. **65**, 634 (1975).
[17] O. Lhagva and L. Hehnmedeh, J. Phys. B **27**, 4623 (1994).
[18] A. S. Kheifets, J. Phys. B **26**, 2053 (1993).
[19] R. J. Tweed and J. Langlois, J. Phys. B **20**, 5213 (1987).
[20] O. Lhagva, Z. Phys. D **23**, 321 (1992).
[21] A. Derevianko, W. R. Johnson, and K. T. Cheng, At. Data Nucl. Data Tables **73**, 153 (1999).
[22] M. Ya. Amusia, A. S. Baltenkov, L. V. Chernysheva, Z. Felfli, and A. Z. Msezane, Phys. Rev. A **63**, 052506 (2001).
[23] R. D. Cowan, *The Theory of Atomic Structure and Spectra* (University of California Press, Berkeley, 1981).
[24] M.-K. Chen, Phys. Rev. A **60**, 2565 (1999), and references therein.
[25] V. L. Jacobs, Phys. Rev. A **10**, 499 (1974).
[26] M. Inokuti, Rev. Mod. Phys. **43**, 297 (1971).
[27] N. L. S. Martin, D. B. Thompson, R. P. Bauman, and M. Wilson, Phys. Rev. Lett. **72**, 2163 (1994).